J. Fluid Mech. (1993), *vol.* 248, *pp.* 383–401

Multiple large-scale coherent mode interactions in a developing round jet

By SANG SOO LEE† AND J. T. C. LIU
Division of Engineering, Brown University, Providence, R.I. 02912, USA

(Received 21 April 1992 and in revised form 23 September 1992)

The integral energy method has been used to study the nonlinear interactions of the large-scale coherent structure in a spatially developing round jet. The streamwise development of a jet is obtained in terms of the mean flow shear-layer momentum thickness, the wave-mode kinetic energy and the wave-mode phase angle. With the energy method, a system of partial differential equations is reduced to a system of ordinary differential equations. The nonlinear differential equations are solved with initial conditions which are given at the nozzle exit. It is shown that the initial wave-mode energy densities as well as the initial phase angles play a significant role in the streamwise evolution of the large-scale coherent wave modes and the mean flow.

1. Introduction

The existence of large-scale coherent structure in a round jet has been well established by many investigations. Several reviews on the large-scale structures in a free shear layer and a round jet are available, including the recent ones by Liu (1988, 1989) and Mankbadi (1992).

It is believed that the helical large-scale coherent mode plays an important role in the development of a round jet. Moore (1977) noticed that the axisymmetric and first-order helical modes were definitely present in a natural round jet at all subsonic velocities. Drubka (1981) was also able to see three-dimensional structures in the initial developing region of a jet. In their flow visualization studies, Dimotakis, Miake-Lye & Papantoniou (1983) observed large-scale structures which were axisymmetric, or helical, or existed in a transitional state between those two configurations, in the fully developed region of turbulent jets.

Experimental and theoretical studies of a round jet by Fuchs (1974) and Michalke & Fuchs (1975) demonstrated the dominance of the first three to four helical modes in the pressure fluctuations. Measurements of the pressure fluctuations of the helical modes were given by Chan (1977). Strange (1981) showed that the axisymmetric and first-order helical modes had comparable growth rates in the initial region of a jet, and the turbulence levels in the shear layer were increased noticeably when the jet was forced with helical modes. From measurements of the near-field pressure and velocities, Drubka (1981) and Drubka, Reisenthel & Nagib (1989) showed that a jet was unstable both for the axisymmetric and helical modes. By using short-time spectral estimates, Corke, Shakib & Nagib (1991) showed that the axisymmetric and helical fundamental modes did not exist at the same time or space. They showed that there was an apparent non-deterministic switching between these modes.

The energy method was first given by Stuart (1958) for a nonlinear stability

† Present address: Sverdrup Technology, Inc., MS 5-9, NASA Lewis Research Center Group, Cleveland, OH 44135, USA.

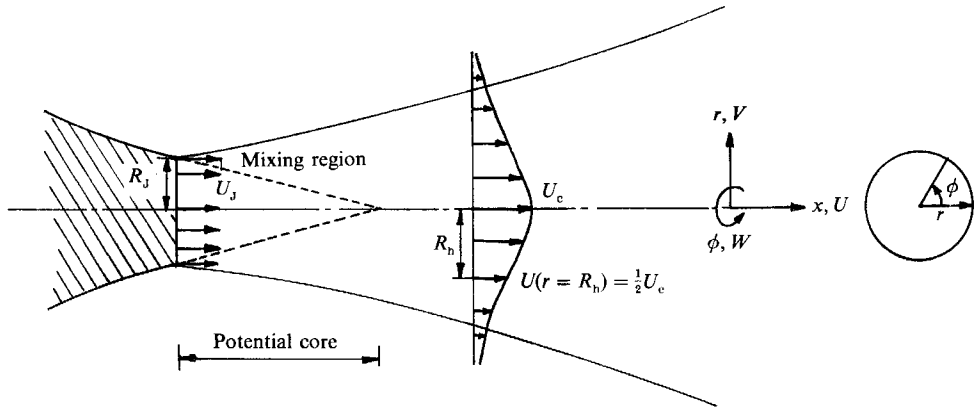

FIGURE 1. Diagram of the initial region of a round jet.

analysis. This method was used by Ko, Kubota & Lees (1970) in the analysis of the nonlinear development of a laminar wake. An application of the energy method to a round jet problem was done by Mankbadi & Liu (1981). The flow field was split into the mean flow, a monochromatic component of a large-scale structure, and fine-grained turbulence. Mankbadi (1985) studied the nonlinear interactions between the axisymmetric large-scale coherent structures. He showed that the predicted results were in good agreement with experimental measurements.

In this study, a formulation and results for the large-scale coherent wave-mode interactions in a spatially developing round jet will be presented. A flow quantity is assumed to be composed of two major components: the mean flow quantity and the large-scale coherent structure. We assume that the jet is artificially excited. Because we are interested in the initial developing region of a jet whose initial turbulence level is low, the effect of the fine-grained turbulence will be excluded from consideration. The large-scale structure is decomposed into five wave modes: axisymmetric, first-order helical and second-order helical fundamental modes, and axisymmetric and first-order helical subharmonic modes. The helical wave modes are included because there is experimental and theoretical evidence which shows that a jet can carry those modes as well as the axisymmetric modes. These five modes still belong to the family of binary-frequency interactions (Nikitopoulos & Liu 1987). The interactions among the mean flow and the wave modes, and among the wave modes themselves (between axisymmetric modes, between axisymmetric and helical modes, and between helical modes) will be studied by using the energy method.

With the energy method, a system of partial differential equations is reduced to a system of ordinary differential equations. The nonlinear differential equations are solved with initial conditions which are given at the nozzle exit. In contrast to the local linear stability theory or weakly nonlinear theory, the streamwise evolution of the mean flow momentum thickness and the amplitudes of the wave modes will be calculated simultaneously in this study.

2. Formulation

The problem considered here is that of a large Reynolds number round jet emitted into still air. The mean flow is assumed to be axisymmetric. The coordinate system used, as shown in figure 1, has x, r, and ϕ as the streamwise, radial and azimuthal directions respectively, and u, v, and w are the corresponding velocity components.

All flow quantities are non-dimensionalized by the nozzle exit radius, R_J, and the jet exit mean velocity, U_J. The Reynolds number is defined as $Re = U_J R_J/\nu$, where ν is the kinematic viscosity.

The interactions between the mean flow and the large-scale coherent structure have been studied by applying conditional and time averaging techniques to the flow quantities (Liu 1988, 1989). The usual time average is slightly modified for our purpose to

$$Q(\boldsymbol{x}) = \lim_{T\to\infty} \frac{1}{2\pi T} \int_0^{2\pi} \int_0^T q(\boldsymbol{x}, t)\, \mathrm{d}t\, \mathrm{d}\phi. \tag{1}$$

Without fine-grained turbulence (Nikitopoulos & Liu 1987), each flow quantity is split into two components: a steady mean flow quantity and a large-scale coherent structure:

$$q(\boldsymbol{x}, t) = Q(\boldsymbol{x}) + \tilde{q}(\boldsymbol{x}, t). \tag{2}$$

The large-scale structure is considered to grow and decay spatially and to be periodic in time and the azimuthal direction. The large-scale velocity components and pressure are decomposed into five wave modes:

$$\tilde{u} = \tilde{u}_{10} + \tilde{u}_{20} + \tilde{u}_{11} + \tilde{u}_{21} + \tilde{u}_{22}, \tag{3}$$

$$\tilde{v} = \tilde{v}_{10} + \tilde{v}_{20} + \tilde{v}_{11} + \tilde{v}_{21} + \tilde{v}_{22}, \tag{4}$$

$$\tilde{w} = \tilde{w}_{11} + \tilde{w}_{21} + \tilde{w}_{22}, \tag{5}$$

$$\tilde{p} = \tilde{p}_{10} + \tilde{p}_{20} + \tilde{p}_{11} + \tilde{p}_{21} + \tilde{p}_{22}, \tag{6}$$

where

$$\begin{pmatrix} \tilde{u}_{mn} \\ \tilde{v}_{mn} \\ \tilde{p}_{mn} \end{pmatrix} = \begin{pmatrix} u'_{mn} \\ v'_{mn} \\ p'_{mn} \end{pmatrix} \mathrm{e}^{-\mathrm{i}m\beta t} \cos n\phi + \text{c.c.}, \tag{7}$$

$$\tilde{w}_{mn} = w'_{mn}\, \mathrm{e}^{-\mathrm{i}m\beta t} \sin n\phi + \text{c.c.}, \tag{8}$$

where c.c. denotes the complex conjugate, and $m\beta$ is the frequency of the wave mode mn. The second subscript n is the azimuthal wavenumber. A wave mode is axisymmetric if n is equal to zero, and helical otherwise. For simplicity we consider only the standing helical modes. The wave modes 20, 21 and 22 are called fundamentals and the 10 and 11 modes are called subharmonics. It can be seen that the wave modes 20, 21 and 22 arise from direct quadratic interaction between the 10 and 11 modes. These five modes still belong to the family of binary-frequency interactions considered in Nikitopoulos & Liu (1987) and are consistent with those used by Stuart (1962). We model an artificially excited jet where the various azimuthal modes are correlated.

3. Shape assumption

3.1. *Mean flow*

By following previous works by Mankbadi & Liu (1981) and Mankbadi (1985), a hyperbolic tangent mean velocity profile which was proposed by Michalke (1971) will be used to represent the mean flow in the initial developing region of a jet:

$$U(r) = \frac{1}{2}\left[1 + \tanh\left(\frac{1}{4\theta}\left(\frac{1}{r} - r\right)\right)\right] \quad \text{for} \quad 0 \leqslant r \leqslant \infty, \tag{9}$$

where θ is the local momentum thickness defined as

$$\theta = \int_0^\infty U(1-U)\,\mathrm{d}r. \tag{10}$$

With the mean velocity profile in (9), the mean flow is parameterized by the momentum thickness only. As a result, the radial integrals involved in the integral equations can be obtained for a given θ instead of a given x. From now on, θ is treated as the independent variable, replacing x, as far as the radial integrals are considered.

The velocity profile (9) has been confirmed by experiments (for example, Strange 1981) and has been successfully used for the investigation of the jet instability in the potential core region (reviewed by Michalke 1984) although it is not self-similar. Monkewitz & Sohn (1988) proposed a more consistent mean flow profile, however, they showed that the results of the stability calculation using their profile were in good agreement with those using the profile (9).

3.2. *Large-scale coherent structure*

A shape assumption in the form of a travelling wave for the large-scale coherent structure is made by following previous works (Liu 1988, 1989). With the decomposition as shown in (3)–(6), the Fourier coefficients in (7) and (8) are assumed to be separable into an unknown finite amplitude and radial shape functions. The shape assumptions for wave mode mn are

$$\begin{pmatrix}\tilde{u}_{mn}\\ \tilde{v}_{mn}\\ \tilde{p}_{mn}\end{pmatrix} = A_{mn}(x)\,\mathrm{e}^{\mathrm{i}\psi_{mn}(x)}\begin{pmatrix}\hat{u}_{mn}(r)\\ \hat{v}_{mn}(r)\\ \hat{p}_{mn}(r)\end{pmatrix}\exp\left(\mathrm{i}\int_0^x \alpha_{r_{mn}}\,\mathrm{d}\zeta - \mathrm{i}m\beta t\right)\cos(n\phi) + \text{c.c.}, \tag{11}$$

$$\tilde{w}_{mn} = A_{mn}(x)\,\mathrm{e}^{\mathrm{i}\psi_{mn}(x)}\hat{w}_{mn}(r)\exp\left(\mathrm{i}\int_0^x \alpha_{r_{mn}}\,\mathrm{d}\zeta - \mathrm{i}m\beta t\right)\sin(n\phi) + \text{c.c.} \tag{12}$$

The subharmonic frequency is one-half of the fundamental frequency. The radial shape functions, denoted by ($\hat{}$), and the complex wavenumber α are obtained from the local viscous linear stability theory, which is confirmed by the good agreement between the local experimental data and the local inviscid linear stability theory (Strange & Crighton 1983 and Cohen & Wygnanski 1987). The radial shape functions and α are dependent on x because the result of the local linear theory is dependent on θ. The phase angle is introduced because the nonlinear interaction between wave modes is dependent on the phase angle differences between them. The amplitude A_{mn}, the phase angle ψ_{mn} and the momentum thickness θ are determined by solving nonlinear integral equations simultaneously.

We emphasize that the radial shape functions need to be normalized for nonlinear calculations. The magnitude of the linear eigenfunctions of the wave mode mn are normalized in such a way that $2\pi A_{mn}^2$ becomes the kinetic energy content of the mn mode across the jet at a given x position:

$$2\pi A_{mn}^2(x) = \frac{1}{2}\int_0^{2\pi}\int_0^\infty (\overline{\tilde{u}_{mn}^2} + \overline{\tilde{v}_{mn}^2} + \overline{\tilde{w}_{mn}^2})\,r\,\mathrm{d}r\,\mathrm{d}\phi. \tag{13}$$

The arguments of the eigenfunctions are normalized by taking the argument of the complex streamwise eigenfunction at the jet centreline to be equal to zero.

The linear viscous stability equations are solved by a Runge–Kutta method with an orthonormalization technique (Lee 1988).

4. Integral equations

If we apply the boundary-layer approximation to the mean flow equations, multiply by U and integrate over a cross-section of a jet, we will get the integral mean energy equation:

$$\frac{1}{2}\frac{\mathrm{d}}{\mathrm{d}x}\int_0^\infty U^3 r\,\mathrm{d}r = -\frac{1}{Re}\int_0^\infty \left(\frac{\partial U}{\partial r}\right)^2 r\,\mathrm{d}r + \int_0^\infty \overline{\tilde{u}\tilde{v}}\frac{\partial U}{\partial r} r\,\mathrm{d}r, \tag{14}$$

where the Reynolds stress term becomes

$$\overline{\tilde{u}\tilde{v}} = \overline{\tilde{u}_{10}\tilde{v}_{10}} + \overline{\tilde{u}_{20}\tilde{v}_{20}} + \overline{\tilde{u}_{11}\tilde{v}_{11}} + \overline{\tilde{u}_{21}\tilde{v}_{21}} + \overline{\tilde{u}_{22}\tilde{v}_{22}}. \tag{15}$$

The term on the left-hand side of (14) represents the advection of the mean flow energy, the first term on the right-hand side represents the viscous dissipation, and the last term represents the energy exchange between the mean flow and the large-scale wave modes.

The integral energy equation of the wave mode mn is obtained by multiplying the wave mode velocity components by their corresponding momentum equations, adding them together, taking the time average of the sum and integrating over a cross-section of the jet:

$$\begin{aligned}\frac{1}{2}\frac{\mathrm{d}}{\mathrm{d}x}\int_0^\infty \overline{\tilde{q}_{mn}^2}\, U r\,\mathrm{d}r = &-\int_0^\infty \overline{\tilde{u}_{mn}\tilde{v}_{mn}}\frac{\partial U}{\partial r} r\,\mathrm{d}r - \frac{\mathrm{d}}{\mathrm{d}x}\int_0^\infty \overline{\tilde{u}_{mn}\tilde{p}_{mn}}\, r\,\mathrm{d}r \\ &-\frac{1}{Re}\int_0^\infty \left[\left(\overline{\left(\frac{\partial \tilde{q}_{mn}}{\partial x}\right)^2} + \overline{\left(\frac{\partial \tilde{q}_{mn}}{\partial r}\right)^2} + \frac{1}{r^2}\overline{\left(\frac{\partial \tilde{q}_{mn}}{\partial \phi}\right)^2}\right)\right. \\ &\left. + \frac{1}{r^2}\left(\overline{\tilde{v}_{mn}^2} + \overline{\tilde{w}_{mn}^2} + \overline{4\tilde{v}_{mn}\frac{\partial \tilde{w}_{mn}}{\partial \phi}}\right)\right] r\,\mathrm{d}r + WW_{mn},\end{aligned} \tag{16}$$

where

$$\tilde{q}_{mn}^2 \equiv \tilde{u}_{mn}^2 + \tilde{v}_{mn}^2 + \tilde{w}_{mn}^2, \tag{17}$$

$$\left(\frac{\partial \tilde{q}_{mn}}{\partial x_i}\right)^2 \equiv \left(\frac{\partial \tilde{u}_{mn}}{\partial x_i}\right)^2 + \left(\frac{\partial \tilde{v}_{mn}}{\partial x_i}\right)^2 + \left(\frac{\partial \tilde{w}_{mn}}{\partial x_i}\right)^2, \tag{18}$$

and $(x_1, x_2, x_3) = (x, r, \phi)$. The mode–mode energy exchange terms are:

$$WW_{10} = -W_{10}W_{10}W_{20} + W_{11}W_{21}W_{10} - W_{10}W_{11}W_{21}, \tag{19}$$

$$WW_{20} = W_{10}W_{10}W_{20} + W_{11}W_{11}W_{20}, \tag{20}$$

$$WW_{11} = -W_{11}W_{10}W_{21} - W_{11}W_{21}W_{10} - W_{11}W_{11}W_{20} - W_{11}W_{11}W_{22}, \tag{21}$$

$$WW_{21} = W_{10}W_{11}W_{21} + W_{11}W_{10}W_{21}, \tag{22}$$

$$WW_{22} = W_{11}W_{11}W_{22}, \tag{23}$$

where

$$\begin{aligned}W_{ij}W_{kl}W_{mn} = \int_0^\infty \left[\overline{\tilde{u}_{ij}\tilde{u}_{kl}\frac{\partial \tilde{u}_{mn}}{\partial x}} + \overline{\tilde{v}_{ij}\tilde{u}_{kl}\frac{\partial \tilde{v}_{mn}}{\partial x}} + \overline{\tilde{w}_{ij}\tilde{u}_{kl}\frac{\partial \tilde{w}_{mn}}{\partial x}}\right. \\ + \overline{\tilde{u}_{ij}\tilde{v}_{kl}\frac{\partial \tilde{u}_{mn}}{\partial r}} + \overline{\tilde{v}_{ij}\tilde{v}_{kl}\frac{\partial \tilde{v}_{mn}}{\partial r}} + \overline{\tilde{w}_{ij}\tilde{v}_{kl}\frac{\partial \tilde{w}_{mn}}{\partial r}} \\ + \frac{1}{r}\left(\overline{\tilde{u}_{ij}\tilde{w}_{kl}\frac{\partial \tilde{u}_{mn}}{\partial \phi}} + \overline{\tilde{v}_{ij}\tilde{w}_{kl}\frac{\partial \tilde{v}_{mn}}{\partial \phi}} + \overline{\tilde{w}_{ij}\tilde{w}_{kl}\frac{\partial \tilde{w}_{mn}}{\partial \phi}}\right. \\ \left.\left. + \overline{\tilde{w}_{ij}\tilde{w}_{kl}\tilde{v}_{mn}} - \overline{\tilde{v}_{ij}\tilde{w}_{kl}\tilde{w}_{mn}}\right)\right] r\,\mathrm{d}r.\end{aligned} \tag{24}$$

The term on the left-hand side of (16) represents the advection of the energy of the wave mode mn by the mean flow. The first term on the right-hand side represents the production of the wave mode energy by the work of the mean flow on the Reynolds stress. It can be observed that the same term appears in the integral mean energy equation (14) with an opposite sign. The second term on the right-hand side represents the pressure work. The third term on the right-hand side represents the viscous dissipation of the kinetic energy of the wave mode. The last term in (16) represents the energy exchange between wave modes.

The triple correlation term $W_{ij}W_{kl}W_{mn}$ represents the energy exchange between wave modes ij and mn. For example, if $W_{10}W_{10}W_{20}$ is positive, there is a net energy transfer from wave mode 10 to wave mode 20. It is shown in (19)–(23) that the term $W_{ij}W_{kl}W_{mn}$ appears in WW_{ij} and WW_{mn} with opposite signs, and the sum of the five WW_{mn} is zero. The third wave mode kl is necessary for the energy exchange between the ij and mn modes.

The phase angle equation of wave mode mn is obtained by

$$[u'^{*}_{mn}(u'_{mn}\text{ momentum equation})-u'_{mn}(u'_{mn}\text{ momentum equation})^{*}]+\ldots \quad (25)$$

where * denotes the complex conjugate. A complete phase angle equation can be found in Lee (1988).

5. Nonlinear analysis

If we substitute the shape assumptions (9), (11) and (12) into the integral equations (14) and (16) and the integral phase angle equation, we can obtain a system of coupled nonlinear ordinary differential equations:

$$\frac{\mathrm{d}\theta}{\mathrm{d}x}\frac{\mathrm{d}}{\mathrm{d}\theta}I_{aM} = -\Phi_M - E_{MW}, \quad (26)$$

$$\frac{\mathrm{d}E_{mn}}{\mathrm{d}x}I_{apWmn} = E_{MWmn} - \Phi_{Wmn} + WW_{mn}, \quad (27)$$

$$\frac{\mathrm{d}\psi_{mn}}{\mathrm{d}x}P_{Amn} = P_{Bmn}+P_{Cmn}+P_{Dmn}+P_{Emn}+PP_{mn}, \quad (28)$$

where

$$E_{MW} = E_{MW10}+E_{MW20}+E_{MW11}+E_{MW21}+E_{MW22}, \quad (29)$$

$$I_{apWmn} = I_{aWmn}+I_{pWmn}, \quad (30)$$

and $E_{mn} \equiv A^2_{mn}$.

The mean flow energy advection integral is

$$I_{aM} = \frac{1}{2}\int_0^\infty U^3 r\,\mathrm{d}r, \quad (31)$$

and the mean flow viscous dissipation integral is

$$\Phi_M = \frac{1}{Re}\int_0^\infty \left(\frac{\mathrm{d}U}{\mathrm{d}r}\right)^2 r\,\mathrm{d}r. \quad (32)$$

The mean flow viscous dissipation term becomes very small for a large Reynolds number jet, and, therefore, the momentum thickness growth is mainly governed by the energy transfer between the mean flow and the wave modes.

The wave-mode energy advection integral is

$$I_{aWmn} = \begin{cases} \int_0^\infty (|\hat{u}_{mn}|^2 + |\hat{v}_{mn}|^2)\, Ur\, \mathrm{d}r & \text{if} \quad n = 0, \\ \frac{1}{2}\int_0^\infty (|\hat{u}_{mn}|^2 + |\hat{v}_{mn}|^2 + |\hat{w}_{mn}|^2)\, Ur\, \mathrm{d}r & \text{if} \quad n \neq 0, \end{cases} \tag{33}$$

and the wave-mode pressure work integral is

$$I_{pWmn} = \lambda \int_0^\infty \mathrm{Re}\,(\hat{u}_{mn}\hat{p}^*_{mn})\, r\, \mathrm{d}r, \tag{34}$$

where $\lambda = 2$ if $n = 0$ and $\lambda = 0$ otherwise and Re is the real part of the complex quantity. The wave-mode viscous dissipation term is

$$\Phi_{Wmn} = E_{mn} I_{vWmn}, \tag{35}$$

where I_{vWmn} can be obtained from (16). The term E_{MWmn} represents the energy exchange between the mean flow and wave mode mn, and is defined as

$$E_{MWmn} = E_{mn} I_{MWmn}, \tag{36}$$

where the wave-mode production integral is

$$I_{MWmn} = -\lambda \int_0^\infty \mathrm{Re}\,(\hat{u}_{mn}\hat{v}^*_{mn}) \frac{\mathrm{d}U}{\mathrm{d}r}\, r\, \mathrm{d}r, \tag{37}$$

and $\lambda = 2$ if $n = 0$ and $\lambda = 1$ if $n \neq 0$. The mode–mode energy exchange term WW_{mn} is given in (19)–(23) and the triple correlation term becomes

$$W_{ij}\, W_{kl}\, W_{mn} = 2\,\mathrm{Re}\,(T_{ij}\, T_{kl}\, T_{mn}), \tag{38}$$

where

$$T_{ij}\, T_{kl}\, T_{mn} = (E_{ij} E_{kl} E_{mn})^{\frac{1}{2}} |I_{ij} I_{kl} I_{mn}| \exp\,(\mathrm{i} f_{ij} f_{kl} f_{mn}), \tag{39}$$

and $I_{ij} I_{kl} I_{mn}$ and $f_{ij} f_{kl} f_{mn}$ can be obtained from (24). It is clear from (38) and (39) that the nonlinear mode–mode energy exchange terms are strongly dependent on the phase angle differences between wave modes.

The terms in the phase angle equation (28) are

$$P_{Amn} = E_{mn} I_{aWmn}, \tag{40}$$

$$P_{Bmn} = E_{mn} \beta_{mn}, \tag{41}$$

$$P_{Cmn} = E_{mn} I_{Cmn}, \tag{42}$$

$$P_{Dmn} = E_{mn} I_{Dmn}, \tag{43}$$

$$P_{Emn} = \frac{dE_{mn}}{dx} I_{Emn}, \tag{44}$$

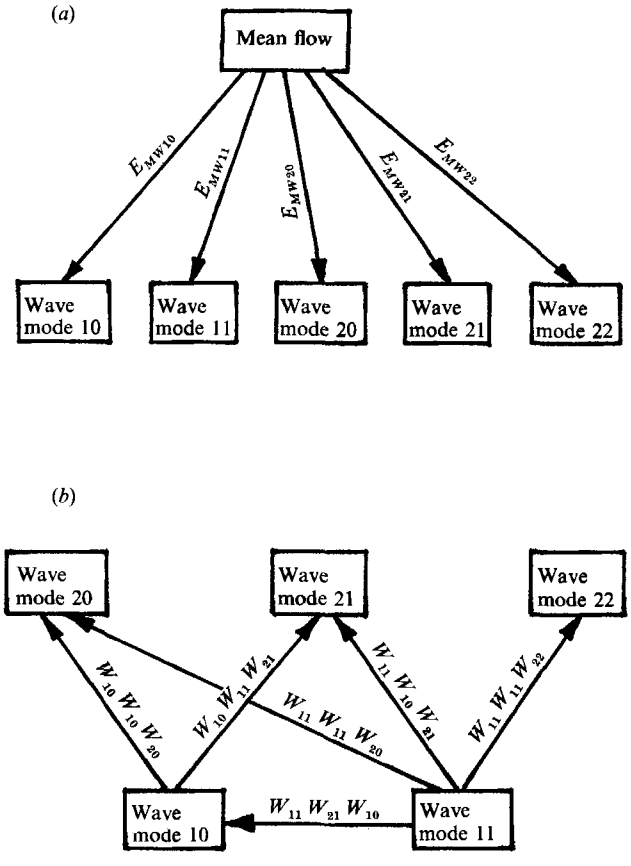

FIGURE 2. Diagrams of the nonlinear energy exchanges: (*a*) between the mean flow and the wave modes; (*b*) between the wave modes.

where the radial integrals are

$$I_{Cmn} = -\alpha_{r_{mn}} I_{aWmn}, \tag{45}$$

$$I_{Dmn} = \frac{\lambda}{2}\int_0^\infty \mathrm{Im}\,(\hat{u}_{mn}\hat{v}^*_{mn})\frac{\mathrm{d}U}{\mathrm{d}r} r\,\mathrm{d}r, \tag{46}$$

$$I_{Emn} = \frac{\lambda}{2}\int_0^\infty \mathrm{Im}\,(\hat{u}_{mn}\hat{p}^*_{mn})\, r\,\mathrm{d}r, \tag{47}$$

and $\lambda = 2$ if $n = 0$ and $\lambda = 1$ otherwise. Im is the imaginary part of the complex quantity. For the nonlinear mode–mode interaction term PP_{mn} in (28), see Lee (1988).

The diagrams of the energy exchanges between the mean flow and the wave modes, and between the wave modes themselves are shown in figure 2. The arrow indicates the direction of the energy transfer when E_{MWmn} or $W_{ij}\,W_{kl}\,W_{mn}$ has a positive value.

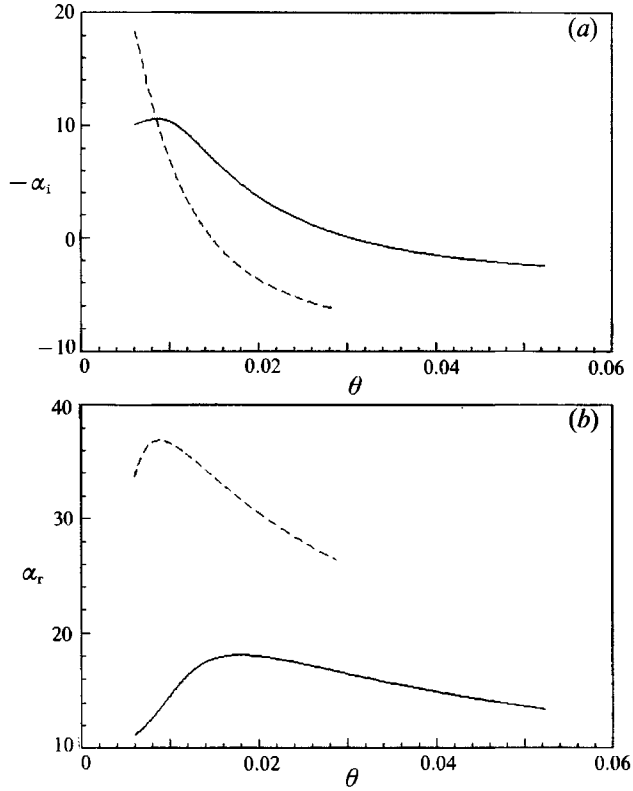

FIGURE 3. (*a*) Amplification rate $-\alpha_i$ and (*b*) wavenumber α_r of axisymmetric wave modes 20 (---, $St_D = 5.54$) and 10 (···, $St_D = 2.77$) versus momentum thickness θ when $Re = 50000$.

6. Results and discussion

The differential equations (26), (27) and (28) are solved simultaneously with initial conditions θ_i, E_{mni} and ψ_{mni}. The streamwise development of a jet will be given in terms of the local shear-layer momentum thickness, the wave-mode energy and the wave-mode phase angle. For all nonlinear calculations, the Reynolds number, based on the nozzle exit radius and mean velocity, is 50000 and the initial shear-layer momentum thickness, non-dimensionalized by the nozzle exit radius, is 0.006. The Strouhal number, based on the nozzle exit diameter ($St_D = fD_J/U_J$, where $D_J = 2R_J$ and f is the frequency), of the fundamental mode is 5.54 ($St_\theta = 0.0166$), and that of the subharmonic mode is 2.77. The frequency of the fundamental mode is the most amplified frequency of the linear viscous stability theory when $Re = 50000$ and $\theta = 0.006$.

The linear amplification rates $-\alpha_i$ and wavenumbers α_r of the axisymmetric wave modes as functions of the local shear-layer momentum thickness are shown in figure 3. The Strouhal number St_D of the fundamental mode 20 is 5.54 and that of the subharmonic mode 10 is 2.77. When $\theta = 0.006$ the amplification rate of the fundamental mode is 18.3 and that of the subharmonic mode is 10.1. The fundamental mode becomes neutral when $\theta = 0.0147$ and the subharmonic mode becomes neutral when $\theta = 0.0303$. The wavenumbers non-dimensionalized by the

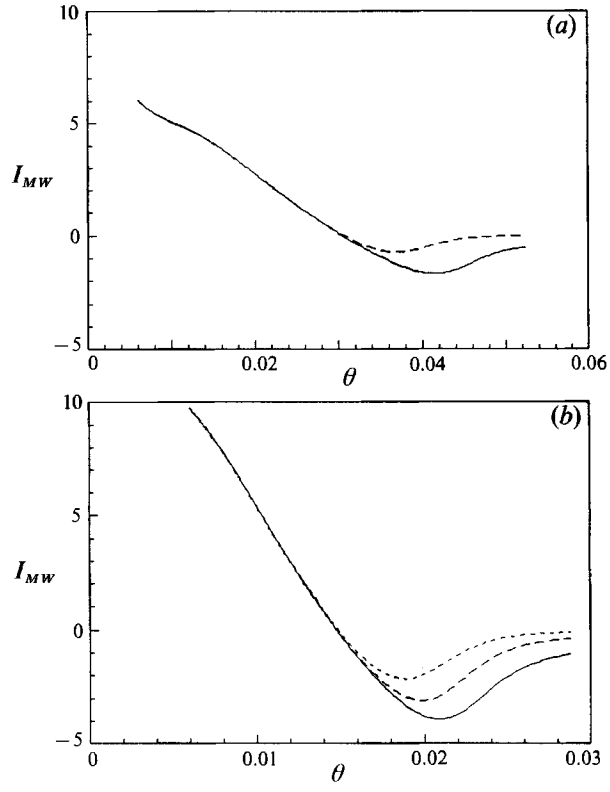

FIGURE 4. Wave-mode production integral I_{MWmn} versus momentum thickness θ; (*a*) subharmonic modes 10 (—) and 11 (---); (*b*) fundamental modes 20 (—), 21 (---) and 22 (· · · ·).

local shear-layer momentum thickness, $\alpha_r \theta$ are 0.202 for the fundamental and 0.067 for the subharmonic when $\theta = 0.006$. It is found that the results for the 20, 21 and 22 modes are almost identical, as are those for the 10 and 11 modes.

The wave-mode production integral I_{MW} is shown in figure 4. The sign of the integral, which indicates the direction of the energy transfer between the mean flow and the wave mode, changes from positive to negative when the wave mode becomes linearly stable ($\theta > 0.0147$ for fundamentals, $\theta > 0.0303$ for subharmonics). The wave mode is amplified by extracting energy from the mean flow in the initial region of a jet and it is damped by returning energy to the mean flow. In the damped region, the helical mode returns less energy to the mean flow than the axisymmetric mode. The phenomenon of changing the direction of the energy transfer, which was first noticed by Ko (1969) in the study of a laminar wake, is now widely observed in the analyses of developing shear flows. A comprehensive discussion about the negative energy production can be found in Liu (1988, 1989).

For given initial values of the total phase angle differences $f_{ij}f_{kl}f_{mni}$, the initial values of the phase angles ψ_{mni} can be determined. From now on, for notational simplicity we will use $fff_i = -\pi$ (or 0) when $f_{11}f_{11}f_{20i} = f_{11}f_{11}f_{22i} = f_{10}f_{11}f_{21i} = f_{11}f_{10}f_{21i} = f_{11}f_{21}f_{10i} = -\pi$ (or 0) and $f_{10}f_{10}f_{20i} = \pi$ (or 2π). A maximum amount of energy will be initially transferred from the fundamentals to the subharmonics when $fff_i = -\pi$.

The streamwise evolution of a jet when E_{mni} (for all five modes) $= 10^{-6}$ and $fff_i = -\pi$ is shown in figures 5 and 6. The shear-layer momentum thickness θ (figure 5)

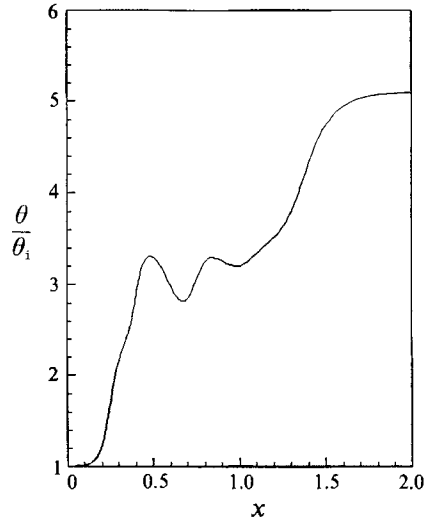

FIGURE 5. Development of the momemtum thickness θ when there are five modes; $E_{10i} = E_{11i} = E_{20i} = E_{21i} = E_{22i} = 10^{-6}$ and $fff_i = -\pi$.

grows when the mean flow loses its kinetic energy. In the early stage of the development of θ where $0 < x < 0.3$, the fundamental energy production terms E_{MW20}, E_{MW21} and E_{MW22} are much larger than the subharmonic terms E_{MW10} and E_{MW11} and the mean flow viscous dissipation term Φ_M. Therefore, the initial growth of θ is mainly governed by the energy transfer from the mean flow to the fundamentals. The growth rate $\mathrm{d}\theta/\mathrm{d}x$ decreases as the fundamental energy production terms decrease, and increases again because of the energy transfer from the mean flow to the subharmonics. The fundamental extracts energy from the mean flow where $0 < x < 0.35$ and returns energy to the mean flow where $x > 0.35$, while the mean flow loses energy to the subharmonics in the whole region. The decreasing value of θ in the regions where $0.48 < x < 0.65$ and $0.85 < x < 1.0$ is due to the negative fundamental energy production. In the downstream region where $x > 1.3$, the effect of the fundamentals on the development of the mean flow is very small and the momentum thickness grows mainly due to the energy transfer from the mean flow to the subharmonics. The effect of the viscous dissipation on the development of the mean flow is negligibly small.

The fundamental energy densities E_{20}, E_{21} and E_{22}, shown in figure 6, grow due to the energy transfer from the mean flow to the fundamentals in the region where $0 < x < 0.3$. In this region, the fundamental energy production terms are much larger than the viscous dissipation terms (Φ_{Wmn}) and the nonlinear mode–mode energy exchange terms (WW_{mn}). As shown in figure 4, the fundamental-mode production integrals I_{MW20}, I_{MW21} and I_{MW22} are almost identical when the wave modes are linearly unstable. As a result, the fundamental energy densities E_{20}, E_{21} and E_{22} grow identically until they reach peak values. The phenomenon is consistent with the experimental observations by Drubka (1981) who showed that the axisymmetric and first-order helical modes grew almost identically in the initial region of jet development. In the region where $x > 0.3$, the nonlinear mode–mode interactions become very strong and the development of the fundamentals is strongly dependent

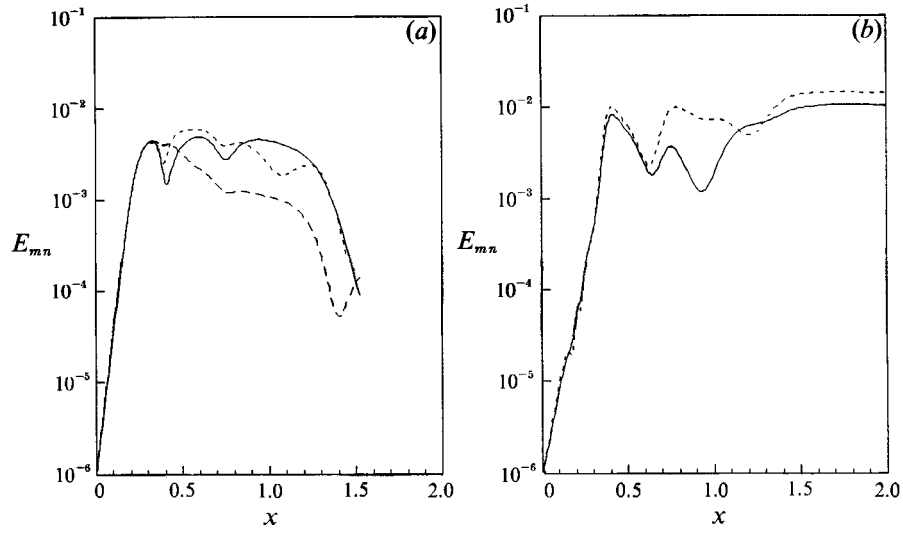

FIGURE 6. Development of the energy densities when there are five modes: (*a*) fundamental energy densities E_{20} (——), E_{21} (· · · ·) and E_{22} (- - -); (*b*) subharmonic energy densities E_{10} (——) and E_{11} (· · · ·); $E_{mni} = 10^{-6}$ and $fff_i = -\pi$.

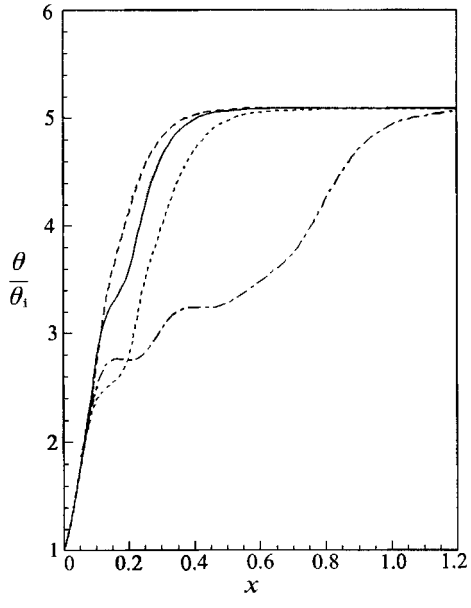

FIGURE 7. Effect of the initial phase angle difference on the development of the momentum thickness θ when $E_{mni} = 10^{-3}$ and $fff_i = -\pi$ (——), $-\frac{1}{2}\pi$ (— · —), 0 (· · · ·) and $\frac{1}{2}\pi$ (- - -).

on the mode–mode energy exchanges. The fluctuations in the streamwise development of the fundamentals, which occur after they are fully grown, have been observed in the experimental studies by Laufer & Zhang (1983) and Drubka (1981). Drubka (1981) also showed that the axisymmetric and first-order helical fundamental modes developed differently after they reached peak values. The subharmonics start to grow at lower growth rates than the fundamentals because they initially

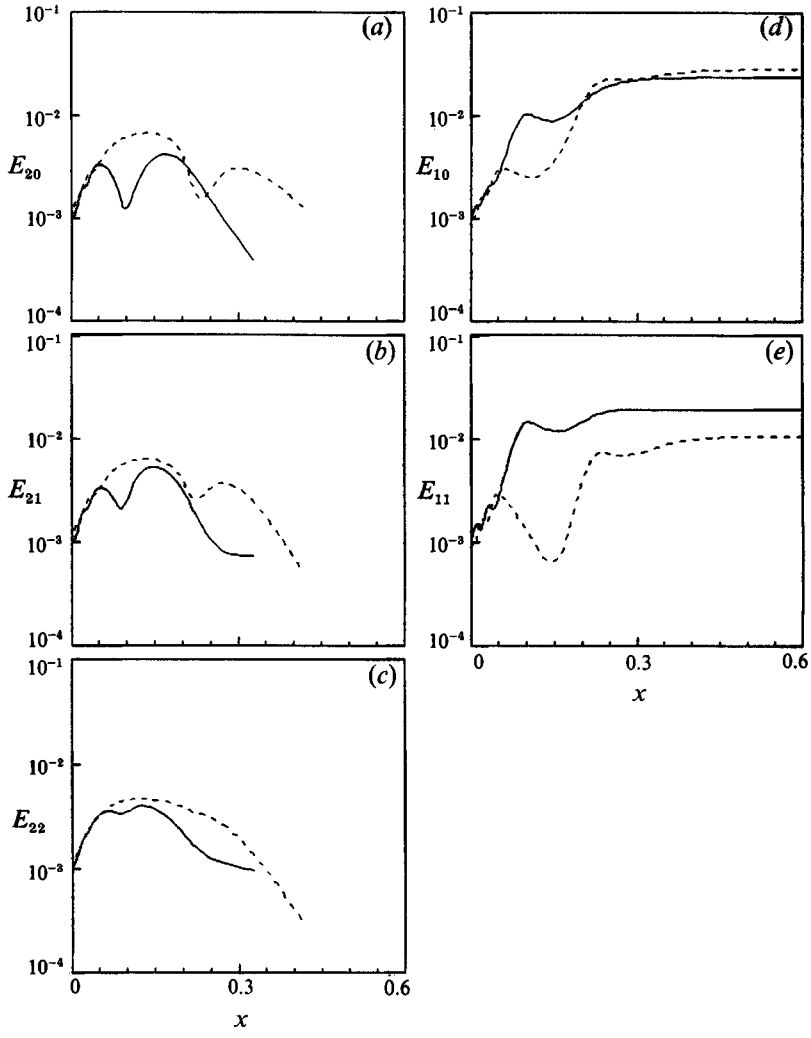

FIGURE 8. Effect of the initial phase angle difference on the development of the energy densities when $E_{mn1} = 10^{-3}$ and $fff_1 = -\pi$ (——) and 0 (· · · ·): (*a*) E_{20}; (*b*) E_{21}; (*c*) E_{22}; (*d*) E_{10}; (*e*) E_{11}.

extract a smaller amount of energy from the mean flow. In the region where $0 < x < 0.3$, there are small fluctuations in the subharmonic energy densities E_{10} and E_{11} because the nonlinear mode–mode energy exchange terms WW_{10} and WW_{11} are comparable with the subharmonic energy production terms E_{MW10} and E_{MW11}. Because of the large amount of energy transferred from the fundamentals to the subharmonics, the growth rates of subharmonics are considerably increased in the region where $0.3 < x < 0.4$.

The result shown in figure 6 is consistent with the experimental result by Corke & Kusek (1993) who studied the mode–mode interaction in a round jet by forcing an axisymmetric mode and helical modes of $n = \pm 1$. The axisymmetric mode was forced at the harmonic frequency of the helical mode. They showed that the axisymmetric mode grew according to the linear stability theory throughout the initial region. However, the initial linear growth of the helical mode was followed by a sharp increase.

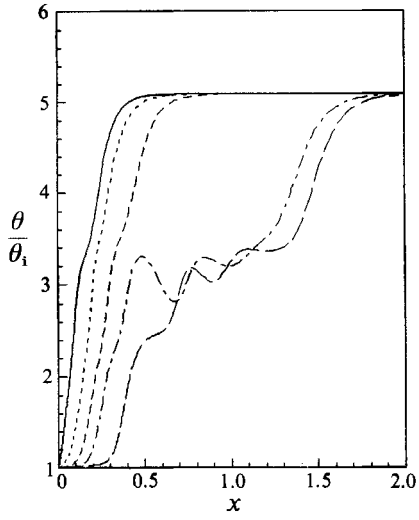

FIGURE 9. Effect of the initial energy density on the development of the momentum thickness θ. $E_{10i} = E_{11i} = E_{20i} = E_{21i} = E_{22i} = 10^{-8}$ (——), 10^{-6} (— · —), 10^{-5} (---), 10^{-4} (· · · ·), and 10^{-3} (——); $fff_i = -\pi$.

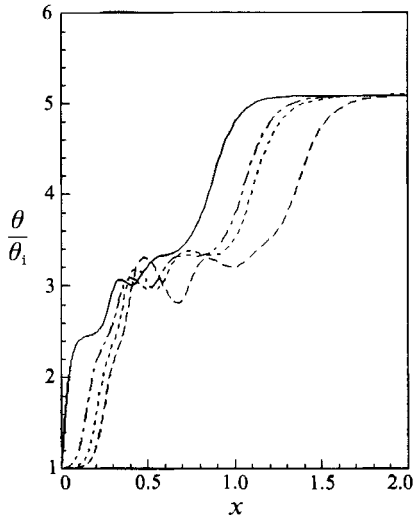

FIGURE 10. Effect of the initial energy density of wave mode 20 on the development of the momentum thickness θ. $E_{20i} = 10^{-6}$ (---), 10^{-5} (· · · ·), 10^{-4} (— · —) and 10^{-2} (——); $E_{10i} = E_{11i} = E_{21i} = E_{22i} = 10^{-6}$; $fff_i = -\pi$.

Figures 7 and 8 show the effect of the initial phase angle difference on the development of a jet when $E_{mni} = 10^{-3}$. Four different values of the initial total phase angle difference, $fff_i = -\pi$, $-\frac{1}{2}\pi$, 0 and $\frac{1}{2}\pi$, are examined. In the initial region of a jet, the different initial values of fff_i do not affect the development of the shear-layer momentum thickness and the fundamental energy densities. However, the initial growth of the subharmonic energy densities is dependent on the initial total phase angle difference. The peak values of the fundamental energy densities when $fff_i = 0$ are greater than those when $fff_i = -\pi$. The shear-layer momentum thickness

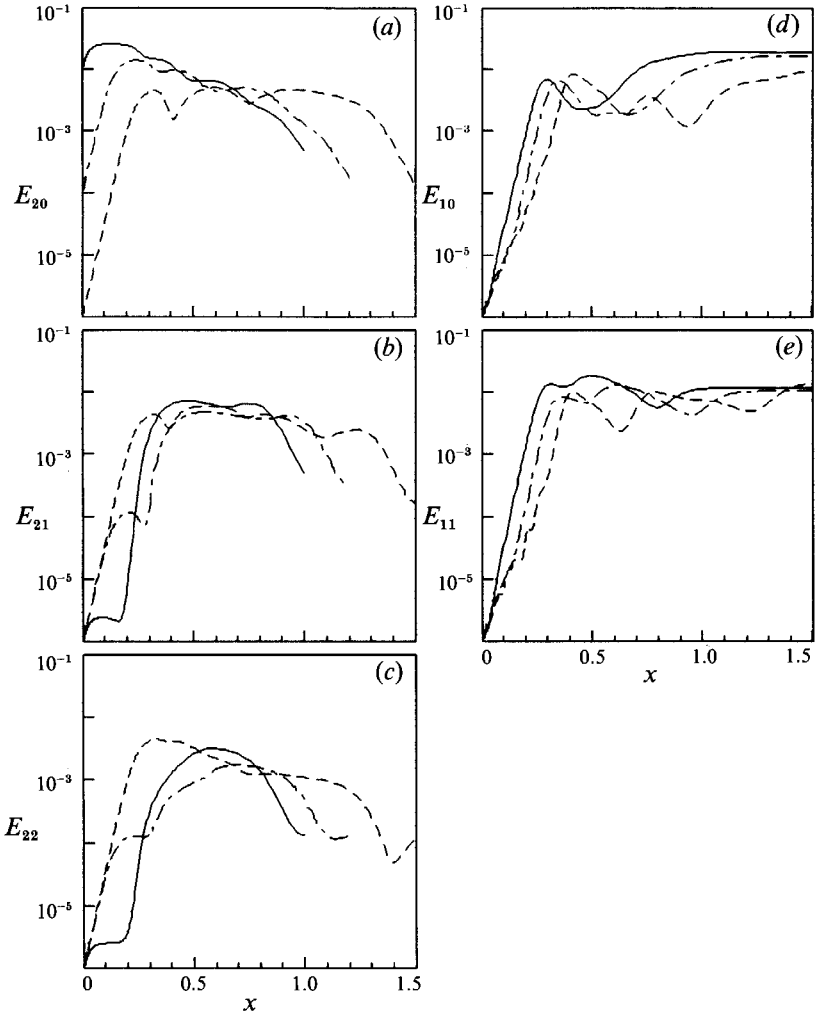

FIGURE 11. Effect of the initial energy density of wave mode 20 on the development of (*a*) E_{20}; (*b*) E_{21}; (*c*) E_{22}; (*d*) E_{10}; (*e*) E_{11}. $E_{20i} = 10^{-6}$ (- - -), 10^{-4} (— · —) and 10^{-2} (——); $E_{10i} = E_{11i} = E_{21i} = E_{22i} = 10^{-6}$; $fff_i = -\pi$.

grows almost monotonically when $fff_i = \frac{1}{2}\pi$. The fastest growth of the momentum thickness is obtained when $fff_i = \frac{1}{2}\pi$.

The effect of the initial energy density on the development of the shear-layer momentum thickness is shown in figure 9. The initial conditions are $fff_i = -\pi$ and E_{mni} ($= E_{10i} = E_{11i} = E_{20i} = E_{21i} = E_{22i}$) $= 10^{-8}$, 10^{-6}, 10^{-5}, 10^{-4} and 10^{-3}. The momentum thickness grows faster when the initial energy density is increased. The peak values of the momentum thickness are not strongly affected by the initial value of the energy density. The delayed growth of the momentum thickness, which is observed in the region where $0.5 < x < 1$ when $E_{mni} = 10^{-6}$ and 10^{-8}, does not occur when the initial energy density is high.

Figures 10 and 11 show the results of the nonlinear analysis when the axisymmetric fundamental mode 20 is forced with different initial values, $E_{20_i} = 10^{-6}$, 10^{-5}, 10^{-4} and 10^{-2}, while the initial energy densities of the other modes are kept constant,

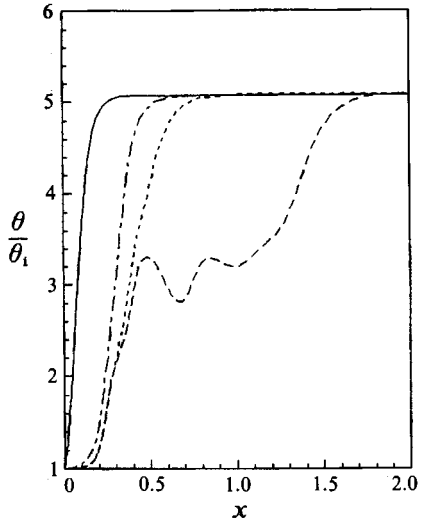

FIGURE 12. Effect of the initial energy density of wave mode 10 on the development of the momentum thickness θ. $E_{10i} = 10^{-6}$ (---), 10^{-5} ($\cdots$), 10^{-4} (— · —) and 10^{-2} (——); $E_{11i} = E_{20i} = E_{21i} = E_{22i} = 10^{-6}$; $fff_i = -\pi$.

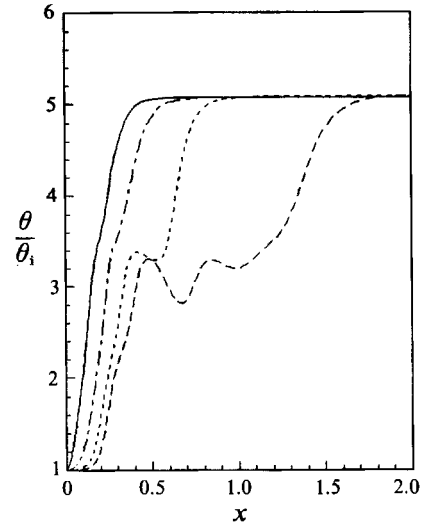

FIGURE 13. Effect of the initial energy densities of axisymmetric modes 10 and 20 on the development of the momemtum thickness θ. $E_{10i} = E_{20i} = 10^{-6}$ (---), 10^{-5} ($\cdots$), 10^{-4} (— · —) and 10^{-3} (—); $E_{11i} = E_{21i} = E_{22i} = 10^{-6}$; $fff_i = -\pi$.

$E_{mni} = 10^{-6}$, and $fff_i = -\pi$. When the initial energy density of the 20 mode is increased, the initial growth rate of the shear-layer momentum thickness is increased and E_{20} reaches a peak value at an earlier streamwise position. When E_{20i} is higher than E_{21i} and E_{22i}, the fast growth of the momentum thickness lessens the total amount of energy transferred from the mean flow to the helical fundamental modes. Therefore, the initial growth rates of E_{21} and E_{22} decrease as E_{20i} increases. When E_{20i} is increased, the subharmonic energy densities grow faster and reach peak values at earlier streamwise positions.

Figure 12 shows the results of the calculations when the axisymmetric subharmonic

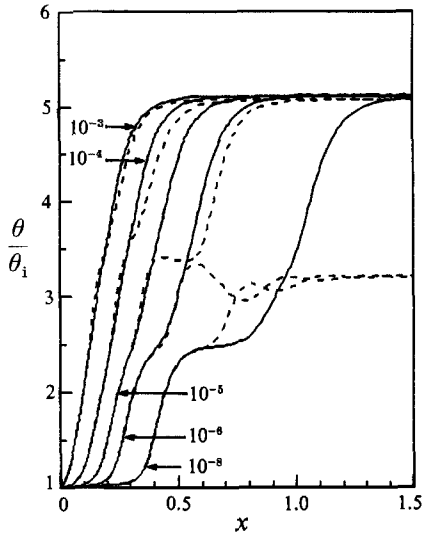

FIGURE 14. Binary-mode interactions; ——, the 10 and 20 mode interaction; ---, the 11 and 22 mode interaction. $E_{10i} = E_{20i}$ (or $E_{11i} = E_{22i}$) = 10^{-8}, 10^{-6}, 10^{-5}, 10^{-4} and 10^{-3}; $f_{10}f_{10}f_{20i}$ (or $f_{11}f_{11}f_{22i}$) = π.

mode 10 is forced with different initial values, $E_{10i} = 10^{-6}$, 10^{-5}, 10^{-4} and 10^{-2}, while the initial values of the other modes, $E_{11i} = E_{20i} = E_{21i} = E_{22i} = 10^{-6}$, and the initial total phase angle difference, $fff_i = -\pi$, are kept constant. When $E_{10i} = 10^{-4}$ the magnitude of E_{MW10}, which represents the energy transfer from the mean flow to the 10 mode, is much greater than the other terms in the integral energy equation. Therefore, the mean flow and the 10 mode grow as if there is only the 10 mode present. In general, when the initial value of the energy density of the 10 mode is larger than the other modes, the other modes do not affect the development of the shear-layer momentum thickness throughout the whole region.

Figure 13 shows the result of the nonlinear analysis when the axisymmetric fundamental mode 20 and subharmonic mode 10 are forced, $E_{10i} = E_{20i} = 10^{-6}$, 10^{-5}, 10^{-4} and 10^{-3}. The initial energy density of the other modes, $E_{11i} = E_{21i} = E_{22i} = 10^{-6}$, and the initial total phase angle difference, $fff_i = -\pi$, are kept constant. When the initial value of the energy densities of the axisymmetric modes is large, the helical modes do not affect the development of θ.

We have shown the results when all of the five modes were initially present. One may need to kill some of the modes in order to understand which type of interaction is important to the control of the mixing rate. Figure 14 shows the results of two binary-mode interactions. The results of the axisymmetric mode interaction, where only the 10 and 20 modes are present, are plotted as the solid curves. The dotted lines depict the results of the interaction when there are only two helical modes, 11 and 22. In the calculation the wave modes are forced with different initial values, $E_{10i} = E_{20i}$ (or $E_{11i} = E_{22i}$) = 10^{-8}, 10^{-6}, 10^{-5}, 10^{-4} and 10^{-3}. The initial total phase angle difference $f_{10}f_{10}f_{20i}$ or $f_{11}f_{11}f_{22i}$ is π. The momentum thickness grows faster in the two-helical-mode interaction than in the two-axisymmetric-mode interaction.

7. Concluding remarks

The results of the five-mode interaction show that the axisymmetric and helical modes grow almost identically in the initial region until the energy densities of the fundamental modes reach peak values. When the initial energy densities of the fundamental and subharmonic modes are equal, the initial growth of the shear-layer momentum thickness and the fundamental energy densities is mainly governed by the energy transfer from the mean flow to the fundamental modes. The subharmonic energy densities reach peak values at earlier or later streamwise positions than in the linear case, depending upon the energy transfer between the fundamental and subharmonic modes. The nonlinear interaction between wave modes is strongly dependent on the phase angle difference between them. It is emphasized that the initial phase angle differences between modes as well as the initial energy densities play a significant role in the streamwise evolution of the mean flow and the large-scale coherent modes.

The present work not only contributes to fundamental understanding of the initial development of a jet but also provides an idea for controlling of a jet. For instance, one can control the jet spreading by optimizing the initial conditions of the wave-mode amplitudes. This has some technical applications, for example in reducing jet noise, improving combustion and reducing emission.

This work is partially supported by the National Science Foundation, Fluid Dynamics and Hydraulics Program through Grant MSM83-20307; the National Aeronautics and Space Administration, Lewis Research Center through Grant NAG3-1016 and the Defense Advanced Research Projects Agency, Applied and Computational Mathematics Program through its University Research Initiative, while monitored by Dr Helena S. Wisniewski. The authors wish to express their gratitude to Dr R. R. Mankbadi, Professor J. T. Stuart, F.R.S., and Professor T. C. Corke for many helpful discussions.

REFERENCES

Chan, Y. Y. 1977 *AIAA J.* **15**, 992–1001.

Cohen, J. & Wygnanski, I. 1987 *J. Fluid Mech.* **176**, 191–219.

Corke, T. C. & Kusek, S. M. 1993 *J. Fluid Mech.* **249**, 307–336.

Corke, T. C., Shakib, F. & Nagib, H. M. 1991 *J. Fluid Mech.* **223**, 253–311.

Dimotakis, P. E., Miake-Lye, R. C. & Papantoniou, D. A. 1983 *Phys. Fluids* **26**, 3185–3192.

Drubka, R. E. 1981 Instabilities in near field of turbulent jets and their dependence on initial conditions and Reynolds number. Ph.D. thesis, Illinois Institute of Technology.

Drubka, R. E., Reisenthel, P. & Nagib, H. M. 1989 *Phys. Fluids* A **1**, 1723–1735.

Fuchs, H. V. 1974 *AGARD Conf. Proc.* **131**, Paper 27.

Ko, D. R. S. 1969 I. Supersonic laminar boundary layer along a two-dimensional adiabatic curved ramp. II. Non-linear stability for a laminar, incompressible wake. Ph.D. thesis, California Institute of Technology.

Ko, D. R. S., Kubota, T. & Lees, L. 1970 *J. Fluid Mech.* **40**, 315–341.

Laufer, J. & Zhang, J. X. 1983 *Phys. Fluids* **26**, 1740–1750.

Lee, S. S. 1988 Multiple coherent mode interaction in a developing round jet. Ph.D. thesis, Brown University.

Liu, J. T. C. 1988 *Adv. Appl. Mech.* **26**, 183–309.

Liu, J. T. C. 1989 *Ann. Rev. Fluid Mech.* **21**, 285–315.

MANKBADI, R. R. 1985 *J. Fluid Mech.* **160**, 385–419.

MANKBADI, R. R. 1992 *Appl. Mech. Rev.* **45**, 219–248.

MANKBADI, R. & LIU, J. T. C. 1981 *Phil. Trans. R. Soc. Lond.* A **298**, 541–602.

MICHALKE, A. 1971 *Z. Flugwiss.* **19**, 319–328.

MICHALKE, A. 1984 *Prog. Aerospace Sci.* **21**, 159–199.

MICHALKE, A. & FUCHS, H. V. 1975 *J. Fluid Mech.* **70**, 179–205.

MONKEWITZ, P. A. & SOHN, K. D. 1988 *AIAA J.* **26**, 911–916.

MOORE, C. J. 1977 *J. Fluid Mech.* **80**, 321–367.

NIKITOPOULOS, D. E. & LIU, J. T. C. 1987 *J. Fluid Mech.* **179**, 345–370.

STRANGE, P. J. R. 1981 Spinning modes in orderly jet structure and jet noise. Ph.D. thesis, University of Leeds.

STRANGE, P. J. R. & CRIGHTON, D. G. 1983 *J. Fluid Mech.* **134**, 231–245.

STUART, J. T. 1958 *J. Fluid Mech.* **4**, 1–21.

STUART, J. T. 1962 *Adv. Aeronaut. Sci.* **3**, 121–142.